

28th Annual CSP Workshop on “Recent Developments in Computer Simulation Studies in Condensed Matter Physics”, CSP 2015

## The effect of surface adsorption on tertiary structure formation in helical polymers

Matthew J. Williams<sup>a,\*</sup>, Michael Bachmann<sup>a,b,c</sup>

<sup>a</sup>Soft Matter Systems Research Group, Center for Simulation Physics, The University of Georgia, Athens, Georgia 30602, USA

<sup>b</sup>Instituto de Física, Universidade Federal de Mato Grosso, 78060-900 Cuiabá (MT), Brazil

<sup>c</sup>Departamento de Física, Universidade Federal de Minas Gerais, 31270-901 Belo Horizonte (MG), Brazil

### Abstract

Formation of tertiary structures made up of helical polymer segments is modified by the introduction of a substrate on which the polymer is adsorbed. The effect of a substrate on biological systems such as helical structures may have been important in the formation of early life. We perform replica-exchange Monte Carlo simulations to study this effect on formation of helical structures in coarse grained polymers – comparing the structural phase space for both adsorbed and non-adsorbed helical polymers. For this purpose a generic, hybrid coarse-grained model for polymer adsorption has been employed.

© 2015 The Authors. Published by Elsevier B.V. This is an open access article under the CC BY-NC-ND license

(<http://creativecommons.org/licenses/by-nc-nd/4.0/>).

Peer-review under responsibility of The Organizing Committee of CSP 2015 Conference

**Keywords:** helical polymers; helix bundles; protein folding; structural phases; conformational transitions; Monte Carlo simulation

### 1. Introduction

Helical geometries are often found in biological polymers. The transition between disordered random coil and ordered helical conformations are found to exhibit features of phase transitions [Poland and Scheraga (1970); Badasyan et al. (2010)]. In polymers of sufficient length tertiary structures composed of several helix bundles are observed [Bereau et al. (2011)]. The organization and stability of these helical bundles is the topic of much discussion [Harris et al. (1994); Irbäck et al. (2000)]. Here we explore the cooperative interactions that dictate tertiary structure formation and stabilization in helix bundles.

We perform Monte Carlo simulations to examine homopolymer models which include a torsional potential associated with dihedral angles as well as a bending potential associated with each bending angle similar to the model used by Rapaport (2002). With the inclusion of a torsional potential and bending potential, helical structures emerge and can contort to form a variety of tertiary structural phases. The phase which is formed is dependent on the energy scale of the torsional potential. In a recent study we found that for weak torsion strength, helical structures form but lack the stability found for conformations in a model with stronger torsion potential [Williams and Bachmann (2015)]. Here

\* Corresponding author.

E-mail addresses: [mjw532@uga.edu](mailto:mjw532@uga.edu) (Matthew J. Williams), [bachmann@smsyslab.org](mailto:bachmann@smsyslab.org), [www.smsyslab.org](http://www.smsyslab.org) (Michael Bachmann).

we investigate helical structures formed with a weak torsion potential which produces unstable structures and study the effect on tertiary structure formation and stability with the inclusion of an adsorbent the polymer can attach to.

## 2. Model and sampling algorithm

We model helical polymers using a standard model for elastic flexible polymers [Bachmann (2014)] with additional torsion, bending, and adsorption potentials. The FENE potential acts between bonded monomers and is given by

$$E_{\text{FENE}} = -\frac{1}{2}KR^2 \log\{1 - [(r - r_0)/R]^2\}, \quad (1)$$

where  $r_0 = 1$ ,  $R = 3/7$ , and  $K = 98/5$ . The Lennard-Jones potential,

$$E_{\text{LJ}} = 4[(\sigma/r)^{12} - (\sigma/r)^6] - U_{\text{shift}} \quad (2)$$

acts only between non-bonded monomers separated by a distance less than  $r_{\text{cutoff}}$ , with  $\sigma = 2^{-1/6}$ ,  $r_{\text{cutoff}} = 2.5\sigma$ , and  $U_{\text{shift}} = 4[(\sigma/r_{\text{cutoff}})^{12} - (\sigma/r_{\text{cutoff}})^6]$ . The torsion potential is used as suggested by Rapaport (2002),

$$E_{\tau} = S_{\tau} [1 - \cos(\tau - \tau_0)] \quad (3)$$

with  $\tau_0 = 0.873$  for all dihedral angles. The bending potential reads

$$E_{\theta} = S_{\theta} [1 - \cos(\theta - \theta_0)] \quad (4)$$

and the reference bending angle  $\theta_0 = 1.4$  induces helix formation [Williams and Bachmann (2015)]. Using a strong bending energy scale of  $S_{\theta} = 200$  allows for the formation of structures with local helical order and global helix bundle order. With the variation of  $S_{\tau}$  we are able to control the number of helices present in the helix bundles. Larger values of  $S_{\theta}$  produce bundles with fewer but more stable helices. At  $S_{\tau} = 6$  we see formation of 3- and 4-helix bundles with varying helical segment alignment at low temperature.

To determine the effect of a substrate that acts as an adsorbent for the polymer we include a potential associated with each monomer's height above the surface. The adsorption energy is calculated by integration of the Lennard-Jones potential over the entire half space of the substrate. The adsorption potential is given by

$$E_A = S_A \left[ \frac{2}{15} \left( \frac{\sigma}{h} \right)^9 - \left( \frac{\sigma}{h} \right)^3 \right], \quad (5)$$

where  $h$  is the distance of a monomer above the surface. In this paper we consider an array of adsorption energy scale parameters between  $S_A = 0$  and 2.

For each model, we simulate at 24 temperatures using parallel tempering – developed and advanced by Geyer (1991), Swendsen and Wang (1986), and Hukushima and Nemoto (1996). During an initial equilibration period, temperature spacing and displacement box sizes are dynamically adjusted to give adequate exchange probability and displacement acceptance rates.

## 3. Structures formed at an array of $S_A$ values

We can see in Fig. 1 that at  $S_A = 0$  polymer structures, while predominately consisting of three-helix bundles at low temperature, exhibit variability in terms of alignment and helix segment length. As the adsorption strength is increased we find that the helical structure forms more consistent tertiary structures over a wide range of temperatures, taking the form of two-helix bundles instead of three.

To classify structures more rigorously we introduce a pair of order parameters ( $q_1$  and  $q_2$ ) which make a distinction between local helical order and globular collapse disorder in a polymer structure. In order parameter space, qualitatively similar structures form distinct clusters. As illustrated in Fig. 2, the parameter  $q_1$  describes the average over all monomers of their total Lennard-Jones interaction with other monomers within 6 or fewer bonds,

$$q_1(\mathbf{X}) = \frac{1}{N} \sum_{i=1}^{N-2} \sum_{j=i+2}^N \Theta_{6,j-i} E_{\text{LJ}}(r_{ij}). \quad (6)$$

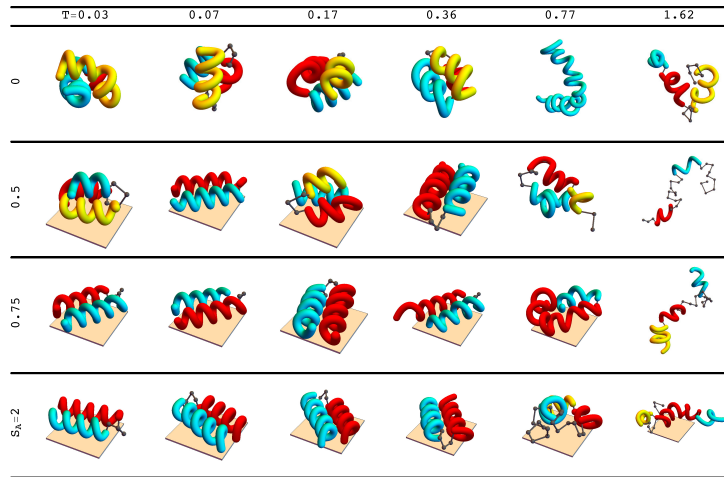


Fig. 1. This figure shows examples of structures formed under varied conditions. Each row shows structures for a single value of  $S_A$  along an array of temperatures between  $T = 0.03$  and  $1.62$ . The adsorption strength increases from top to bottom from a value of  $S_A = 0$  to  $2$ .

Conversely,  $q_2$  is the average over all monomers of their Lennard-Jones interaction with those of distance along the chain of more than 6 bonds,

$$q_2(\mathbf{X}) = \frac{1}{N} \sum_{i=1}^{N-2} \sum_{j=i+2}^N \Theta_{j-i-7} E_{LJ}(r_{ij}). \quad (7)$$

Here we have introduced the symbol

$$\Theta_{kl} = \begin{cases} 1, & k \geq l, \\ 0, & \text{otherwise.} \end{cases} \quad (8)$$

Let us consider two examples to show the usefulness of this parameter pair. In a single long helix all monomers have Lennard-Jones contact with other monomers within 6 bonds along the chain but no contact with monomers outside of this local neighborhood;  $q_1$  is minimal and  $q_2$  maximal. In contrast, for a two-helix bundle local LJ interaction at the joint between the two helix segments is sacrificed for the formation of contacts between monomers belonging to the different segments. These monomers are more than 6 bonds distant along the chain. Therefore, compared to the single-helix case,  $q_2$  decreases at the expense of  $q_1$ . Similarly, higher-order helix bundles can also be distinguished by means of these parameters.

Considering each temperature independently we can calculate the canonical mean  $\langle q_2 \rangle$ . By comparing the different values  $S_A$  on the left in Fig. 3, we can discern the temperatures at which each tertiary structure type occurs. The temperature at which polymers desorb from the surface can be seen by noting the peak in the fluctuation of the distance of the center of mass of the polymer from the substrate ( $dh_{\text{cm}}/dT$ ). Above the desorption temperature we see all of the curves converge to that of the  $S_A = 0$  case.

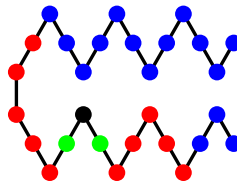


Fig. 2. Black monomer has FENE interaction with nearest neighbor (green) monomers, and Lennard-Jones interaction with all remaining (blue and red) monomers. Lennard-Jones interaction among monomers within a distance of 6 along the polymer chain is distinguished from Lennard-Jones interaction with those of distance along the chain of more than 6. The black monomer interaction with red monomers contributes to  $q_1$  and interaction with blue monomers contributes to  $q_2$ .

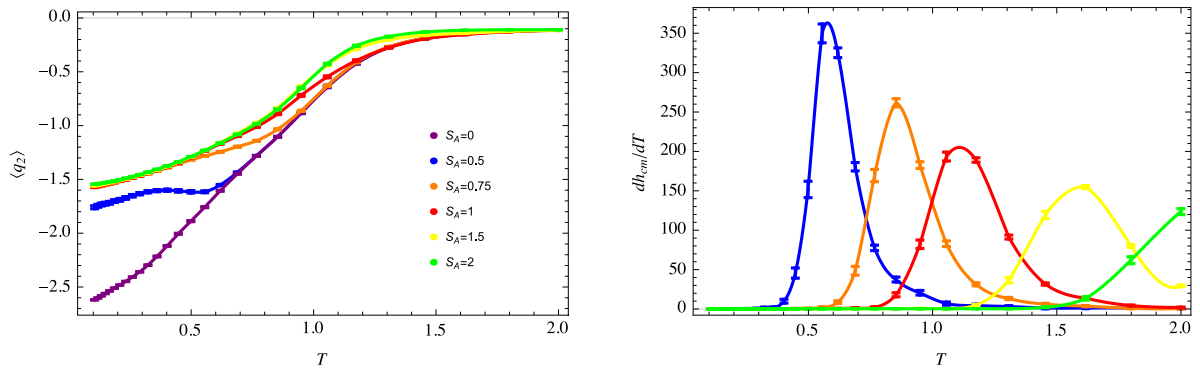


Fig. 3. In the left hand figure we plot  $\langle q_2 \rangle$  as a function of temperature for an array of different values for  $S_A$ . On the right we see the temperature variation of the center of mass distance of polymers at several different adsorption strengths. Note that the peak locations correspond to the temperature at which the polymer desorbs from the surface.

We can better understand the relationship between the ensembles formed at each value of  $S_A$  by considering the structures produced in each of these simulations in  $q_1 - q_2$  space, as seen in Fig. 4. The low-energy structures (produced at low temperature) must in general have lower  $q_1$  and  $q_2$  values, and therefore lie in the lower left hand corner. As we increase  $S_A$  and transition from three-helix to two-helix structures we find that the system sacrifices Lennard-Jones energy from globular collapse in favor of lower energy in the torsion potential and larger contact with the adsorption surface. We see this exhibited by a decrease in  $q_1$  and increase in  $q_2$ .

#### 4. Conclusion

In Fig. 4 we can see that for  $S_A = 0$  or 0.5, structures formed at low temperature are (in the lower left corner) spread out over several unique structure clusters. This indicates that there is instability in the low temperature structure formation. Not only are the structures at both of these values of  $S_A$  unstable, they are also highly sensitive to changes to their environment, as seen by the drastic change in structure type with the introduction of even a weak adsorption

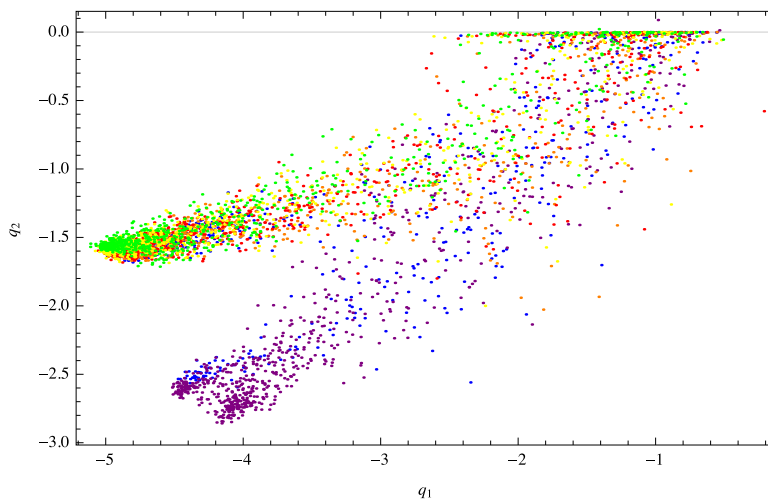


Fig. 4. Shown above is a plot of  $q_1$  vs  $q_2$  for a collection of example structures produced across all temperatures simulated. The color of each point corresponds to the torsion energy scale at which the structure it represents was formed. Structures in  $q_1, q_2$  space cluster with similar structure types. Colors agree with the legend shown in Fig. 3.

surface. Not shown here is their high sensitivity to other changes such as a small change in  $S_T$ . The inherent instability as well as both of these sensitivities is greatly decreased by the inclusion of an adsorption surface as demonstrated by the consistent and single peaked cluster corresponding to two-helix bundles formed for all values of  $S_A$  between 0.75 and 2.0. We infer from these findings that the presence of an adsorption surface stabilizes the tertiary helix bundles formed in a polymer with weak torsional potential.

## Acknowledgements

This work has been supported partially by the NSF under Grant No. DMR-1207437 and by CNPq (National Council for Scientific and Technological Development, Brazil) under Grant No. 402091/2012-4.

## References

- Bachmann, M., 2014. Thermodynamics and statistical mechanics of macromolecular systems. Cambridge University Press.
- Badasyan, A.V., Giacometti, A., Mamasakhlisov, Y.S., Morozov, V.F., Benight, A.S., 2010. Microscopic formulation of the Zimm-Bragg model for the helix-coil transition. *Phys. Rev. E* 81, 021921.
- Bereau, T., Deserno, M., Bachmann, M., 2011. Structural basis of folding cooperativity in model proteins: Insights from a microcanonical perspective. *Biophysical Journal* 100, 2764 – 2772.
- Geyer, C.J., 1991. Markov chain Monte Carlo maximum likelihood, in: Keramidas, E.M. (Ed.), *Computing Science and Statistics, Proceedings of the 23rd Symposium on the Interface* (Interface Foundation, Fairfax, VA, 1991), pp. 156–163.
- Harris, N.L., Presnell, S.R., Cohen, F.E., 1994. Four helix bundle diversity in globular proteins. *Journal of Molecular Biology* 236, 1356 – 1368.
- Hukushima, K., Nemoto, K., 1996. Exchange Monte Carlo method and application to spin glass simulations. *Journal of the Physical Society of Japan* 65, 1604–1608.
- Irbäck, A., Sjunnesson, F., Wallin, S., 2000. Three-helix-bundle protein in a Ramachandran model. *Proceedings of the National Academy of Sciences* 97, 13614–13618.
- Poland, D., Scheraga, H., 1970. Theory of helix-coil transitions in biopolymers: statistical mechanical theory of order-disorder transitions in biological macromolecules. *Molecular Biology*, Academic Press.
- Rapaport, D.C., 2002. Molecular dynamics simulation of polymer helix formation using rigid-link methods. *Phys. Rev. E* 66, 011906.
- Swendsen, R.H., Wang, J.S., 1986. Replica Monte Carlo simulation of spin-glasses. *Physical Review Letters* 57, 2607.
- Williams, M.J., Bachmann, M., 2015. Stabilization of helical biomacromolecular phases by confined bending. Submitted.